Am J Physiol Gastrointest Liver Physiol
279: G1177–G1187, 2000.

Luminal and systemic signals trigger intestinal adaptation in the juvenile python

STEPHEN M. SECOR,[1] EDWARD E. WHANG,[2] JOHN S. LANE,[2]
STANLEY W. ASHLEY,[2] AND JARED DIAMOND[1]
Departments of [1]Physiology and [2]Surgery, School of Medicine,
University of California Los Angeles, Los Angeles, California 90095

Received 26 April 2000; accepted in final form 10 July 2000

Secor, Stephen M., Edward E. Whang, John S. Lane, Stanley W. Ashley, and Jared Diamond. Luminal and systemic signals trigger intestinal adaptation in the juvenile python. *Am J Physiol Gastrointest Liver Physiol* 279: G1177–G1187, 2000.—Juvenile pythons undergo large rapid upregulation of intestinal mass and intestinal transporter activities upon feeding. Because it is also easy to do surgery on pythons and to maintain them in the laboratory, we used a python model to examine signals and agents for intestinal adaptation. We surgically isolated the middle third of the small intestine from enteric continuity, leaving its mesenteric nerve and vascular supply intact. Intestinal continuity was restored by an end-to-end anastomosis between the proximal and distal thirds. Within 24 h of the snake's feeding, the reanastomosed proximal and distal segments (receiving luminal nutrients) had upregulated amino acid and glucose uptakes by up to 15-fold, had doubled intestinal mass, and thereby soon achieved total nutrient uptake capacities equal to those of the normal fed full-length intestine. At this time, however, the isolated middle segment, receiving no luminal nutrients, experienced no changes from the fasted state in either nutrient uptakes or in morphology. By 3 days postfeeding, the isolated middle segment had upregulated nutrient uptakes to the same levels as the reanastomosed proximal and distal segments, but it still lacked any appreciable morphological response. These contrasting results for the reanastomosed intestine and for the isolated middle segment suggest that luminal nutrients and/or pancreatic biliary secretions are the agents triggering rapid upregulation of transporters and of intestinal mass and that systemic nerve or hormonal signals later trigger transporter regulation but no trophic response.

cellular proliferation; digestive response; intestinal hypertrophy; intestinal nutrient transport; regulatory mechanisms

THE CONTROL OF DIGESTION involves exogenous stimuli, leading via signal pathways to tissue responses (e.g., Refs. 4, 21, and 42). Despite nearly a century of effort since Pavlov's pioneering studies of gastrointestinal regulation, much remains to be learned about the underlying mechanisms (12, 23). A practical difficulty limiting progress has been the prevalence of only modest gastrointestinal regulatory spans in the usual laboratory mammalian model species (mice, rats, and rabbits), related to their natural lifestyles of small meals at frequent intervals and hence nearly continuous digestion. Selecting a new model species with large regulatory responses might make it easier to trace gastrointestinal regulatory pathways.

In fact, much larger regulatory responses characterize animal species that normally consume very large meals at infrequent intervals (34). For example, Burmese pythons (*Python molurus*), which consume prey species of body mass up to and exceeding the snake's own body mass at intervals of several weeks or months, undergo a rapid and reversible 2.5-fold increase in intestinal mucosal mass, 6-fold increase in intestinal microvillus length, and up to 50-fold increases in intestinal brush-border nutrient transport, plasma hormone levels, and metabolic rate upon feeding (1, 33, 34). Hence the present paper uses a surgical model to initiate the study of gastrointestinal regulation in pythons.

Ultimate stimuli postulated to trigger postprandial responses of the intestine include the sight of food, smell of food, and gastric distension (21). Postulated proximate regulatory agents include gastrointestinal hormones, nerves, pancreaticobiliary (PB) secretions, and direct contact with luminal nutrients (13, 39, 42). To separate the contributions of some of these stimuli and agents, we have developed a new model of python intestine (similar to Thiry-Vella loops in mammals) in which a segment of intestine is surgically isolated from luminal nutrients and PB secretions while retaining its neural/vascular supply intact. With this model, one can determine whether ultimate cephalic or gastric stimuli can trigger intestinal responses via neural and/or humoral pathways independent of direct stimulation by luminal nutrients or PB secretions. As our assay of response, we compared the surgically isolated segment with the reanastomosed connected segments with respect to nutrient transport rates and mucosal morphology. Because our surgical procedure resulted in the reanastomosed intestine being shorter than a normal intestine, we also measured whether adaptive responses to resection restore the original functional

Address for reprint requests and other correspondence: S. M. Secor, Dept. of Biology, Univ. of Mississippi, P.O. Box 1848, Univ., MS 38677-1848 (E-mail ssecor@olemiss.edu).

The costs of publication of this article were defrayed in part by the payment of page charges. The article must therefore be hereby marked "*advertisement*" in accordance with 18 U.S.C. Section 1734 solely to indicate this fact.

capacity of the shortened intestine, either by proliferation of mucosal mass, increased mass-specific rates of transport, or both. Our results demonstrate the sufficiency of neural and/or hormonal signals for regulating some gastrointestinal responses and also demonstrate the necessity for luminal signals as well in triggering the full suite of gastrointestinal responses.

MATERIALS AND METHODS

Snakes and Experimental Procedures

We bought pythons as 100-g hatchlings from a commercial breeder (Captive Bred Reptiles, Oklahoma City, OK) and maintained them individually in plastic cages on a biweekly diet of laboratory rats, with water available ad libitum. This study used 21 pythons [mean body mass = 1,040 ± 47 (SE) g], equally divided among seven surgical and feeding treatments. Snake body mass did not differ significantly among (ANOVA, $P = 0.87$) or between (planned pair-wise comparisons, $P > 0.16$) treatments. In 18 snakes, we surgically isolated the middle third of the small intestine and reattached the proximal and distal thirds as described in detail below. Out of these 18 snakes, we killed three (by severing the spinal cord immediately posterior to the head) before feeding (after a 60-day fast) and killed three each at 1, 2, 3, 4, and 6 days after consumption of a rat meal equivalent to 25.7 ± 0.6% (snakes killed at 1, 2, 3, and 4 days postfeeding) or 35.2 ± 1.7% (snakes killed at 6 days postfeeding) of the snake's body mass. Because severing and reattaching the small intestine can stimulate intestinal growth and thus potentially increase functional capacity (16), the remaining three snakes served as transected controls; we transected and then immediately reattached their small intestines. These three snakes were killed (after a 60-day fast) without refeeding them. In each snake, we measured nutrient uptake rates across the intestinal brush-border membrane and intestinal mass and morphology, as described below. We compared the results with those previously published (32) for 12 pythons with completely intact intestines (no surgical procedure) and killed at 0, 1, 3, and 6 days after the ingestion of rat meals equaling 25% of body mass (3 snakes/time period). These 12 pythons had been obtained as hatchlings from the same commercial source and were reared in identical conditions as the 21 surgically treated snakes.

Surgical Procedures

Snakes were fasted for 1 mo to ensure that their small intestines were emptied before surgery (32). We anesthetized each snake by placing it within a sealed 4-liter container containing a Halothane-soaked cloth. Complete anesthesia (flaccid body tone and no response to touch) was induced within 5–10 min. Once anesthetized, the snake was laid on its dorsum and held in place with cloth restraints. The scales in the region of the small intestine were scrubbed with Betadine, and a 10-cm incision was made between the ventral scales and first set of lateral scales at a site ~70% of the distance from the snout to the cloaca. The incision was retracted open to expose the middle portion of the small intestine. By gently pulling, we exposed most of the small intestine and thus were able to identify two sites, at approximately one-third and two-thirds of the distance from the pylorus to the large intestine, that divided the small intestine into equal thirds. We then completely transected the small intestine at these two sites while making every effort to minimize disruption of the perpendicular arcade of mesenteric blood vessels and nerves supplying the small intestine. Even though longitudinal enteric blood vessels and nerves must have been severed, the intestine exhibited either no or very little bleeding.

For 18 snakes, the proximal and distal segments of the intestine thus transected into three segments were attached together with an end-to-end anastomosis by a single layer of inverted 4-0 silk sutures, establishing intestinal continuity. We suture-closed both ends of the middle intestinal segment and attached a 10-cm rubber catheter (20 Fr.) through a small hole at the segment's distal end to serve as a drain for any intestinal secretions. The catheter was passed through a small incision in the snake's body wall and was sutured down to external scales. The now-isolated middle segment, with its mesenteric neurovascular supply thus intact, was tucked in along side the reanastomosed proximal and distal segments. For the three transected control snakes, the intestine was transected similarly into three segments, but they were then surgically reattached in their original position.

Finally, the incision through the body wall was closed with an inner (muscular layer) and outer (scales) set of interrupted sutures (3-0 Vicryl; Ethicon). Immediately after surgery, each snake was given a single dose of antibiotic (1 ml/kg enroflovacin; Baytril) intramuscularly, with follow-up injections given at 3-day intervals for the following week and a half. Snakes usually recovered from anesthesia within 1 h and were allowed at least 1 mo of recovery before the start of experiments. During that time, snakes were not fed but were provided with water ad libitum. There was no mortality attributed to the surgical procedure among these 21 snakes.

Intestinal Nutrient Uptake

We measured nutrient uptake rates across the intestinal brush-border membrane in vitro (described in detail in Refs. 25 and 35). We killed the snakes, made a midventral incision the length of the snake, and removed the reanastomosed proximal and distal intestine and the isolated middle intestinal segment. The proximal and distal regions were then cut at the reanastomosis, thus separating the intestine into proximal, middle, and distal segments. Each segment was weighed, flushed with ice-cold Ringer solution, reweighed, everted, and cut into 1-cm sleeves. Sleeves were mounted on glass rods and first were incubated for 5 min in Ringer solution at 30°C and then were incubated for 2 min at 30°C in a Ringer solution containing a radiolabeled nutrient and an adherent fluid marker labeled with a different radioisotope. We measured intestinal uptake rates of the amino acids L-leucine, L-lysine, and L-proline (each at 50 mM and labeled with ^{3}H) and of the sugar D-glucose (at 20 mM and labeled with ^{14}C). These three amino acids are transported predominantly by the neutral, basic, and amino acid transporter, respectively (40). To correct for the amount of radiolabeled nutrient in the fluid adherent to the intestine, we used a second labeled solute: [^{14}C]polyethylene glycol for the amino acids and L-[^{3}H]glucose for D-glucose. In addition, L-[^{3}H]glucose corrects for D-glucose transported via passive diffusion. Thus we measured total uptake (carrier-mediated plus passive) of each amino acid and carrier-mediated uptake of D-glucose. We expressed uptake rates as nanomoles per minute per milligram of sleeve wet mass.

We calculated nutrient uptake capacity (μmol/min) of the reanastomosed small intestine by multiplying uptake rate ($nmol \cdot min^{-1} \cdot mg^{-1}$) times wet mass (mg) for each of the proximal and distal segments and then summed those two products together. After intestinal resection, mammals can restore a portion of the lost functional capacity by adaptation

of the remnant portions (16). We assessed the degree of restoration of functional capacity in a digesting python's intestine, shortened in length by one-third, by comparing our measured nutrient uptake capacities of a reanastomosed intestine with calculated uptake capacities of the same intestine at its original full length. We calculated those original uptake capacities by regressing uptake capacity for each nutrient (log transformed) against log body mass for 19 digesting pythons (1–6 days postfeeding and weighing between 90 and 1,025 g) with fully intact small intestines (Secor and Diamond, unpublished observations). Using the generated regression equations, we used the body mass of each snake in the present study to calculate its original uptake capacity for each nutrient.

Intestinal Morphology

To assess morphological responses of intestinal segments to resection and isolation, we measured for each snake the following four parameters. First, we weighed and averaged the wet masses of five individual 1-cm sleeves taken from each intestinal segment. Second, we used standard light microscopy techniques to measure enterocyte height and width in each intestinal segment. A single 1-cm sleeve from each segment was fixed in 10% neutral-buffered formalin solution, embedded in paraffin, sectioned at 6 μm, and stained with hematoxylin and eosin. For each segment, we averaged the heights and widths (measured using an optical micrometer) and calculated volumes (based on the formula for a cylinder) of 10 randomly selected enterocytes.

Third, we used electron microscopy to measure microvillus lengths from proximal and isolated middle intestinal segments. Small samples of the brush-border membrane were fixed in 4% glutaraldehyde solution, postfixed with 1% osmium tetroxide, dehydrated in a graded series of ethanol, embedded in plastic, sectioned at 90 nm, stained with uranyl acetate and lead, and examined with a Jeol JEM-100 CX electron microscope. For each snake and intestinal segment, we selected one specimen and photographed four or five representative samples of the microvillus border at a magnification of ×7,200. From each print, we measured the length of 10 microvilli, using only microvilli cut in the central plane parallel to their long axis. We calculated actual microvillus length by dividing the length measured from the print by total magnification, and we then averaged lengths for each snake and segment.

Fourth, we used immunohistochemistry techniques employing antiproliferating cell nuclear antigen (anti-PCNA) to identify enterocytes undergoing proliferation. PCNA is a highly conserved nuclear protein (occurring in all eukaryotes) that starts to accumulate during the G1 phase and peaks in abundance during the S phases of the cell cycle. Therefore, it is used as a histological marker to identify cellular proliferation (9). Light microscopy cross-sections (6 μm thick) of proximal, middle, and distal intestinal segments from each snake were mounted on poly-L-lysine-coated glass slides, deparaffinized, dehydrated, and sequentially immersed in 3% H_2O_2 and normal horse serum to block endogenous peroxidase activity and nonspecific binding of secondary antisera, respectively. Anti-PCNA (PC 10, 1:250 dilution; Boehringer Mannheim) was applied overnight, followed the next day by applications of the secondary antisera (biotinylated horse anti-mouse; Vector Laboratories), avidin-biotin complex (Vectastain ABC kit; Vector Laboratories), chromogen (diaminobenzidine), and hematoxylin counterstain. We viewed slides at ×60 magnification and counted the number of labeled and unlabeled cells along a 100-m length of mucosa at five separate positions. As an index of proliferation rates, we calculated the percent of labeled cells (labeled cells/total cells) for each region and averaged those percentages.

Morphological Response of Other Organs

Because gastric hyperplasia has been observed in rats after jejunectomy (36) and because we observed postprandial changes in the masses of several organs in pythons (32), we assessed the effects of intestinal resection and of feeding on the wet and dry masses of the heart, lungs, liver, stomach, pancreas, gallbladder, large intestine, and paired kidneys. Each organ was weighed immediately upon its removal from the snake (wet mass), dried at 60°C for 14 days, and reweighed (dry mass).

Statistical Analyses

We used ANOVA to test for significant effects of intestinal condition (normal, transected, or resected) and sampling time (before and after feeding) on intestinal uptake rates. A repeated-design ANOVA was employed to test for positional effects (proximal, middle, and distal small intestine) within each treatment on nutrient uptake rates. Analysis of covariance (ANCOVA), with body mass as a covariate, was used to test for sampling time effects on uptake capacities of the reanastomosed intestine and on organ masses. In conjunction with ANOVA or ANCOVA, we made a priori planned pair-wise mean comparisons between pairs of treatments. We report results of ANOVAs and ANCOVAs in terms of their F and P values, and we provide P values of significant pair-wise comparisons. We designate the level of statistical significance as $P < 0.05$. Mean values are reported either as means ± SE or as means adjusted for effects of body mass (least-squares means from ANCOVA) ± SE. We conducted all statistical analyses by the microcomputer version of SAS.

RESULTS

Intestinal Nutrient Uptake Rates

We determined whether our surgical procedure influenced intestinal function in fasted snakes by comparing nutrient uptake rates among the following three treatments: normal intact intestine (no surgery), transected intestine, and resected intestine (reanastomosed proximal and distal intestine and isolated middle intestine). Uptake rates of L-leucine, L-lysine, L-proline, and D-glucose did not differ significantly among (ANOVA, mean of P values = 0.49) or between (pair-wise comparisons, mean of P values = 0.51) these three treatments for the proximal, middle, or distal segments; however, there was one exception: L-lysine uptake by distal segments was greater in transected intestines than in normal intestines (Fig. 1). There were also no significant differences in any measured morphological parameters among these three treatments. Thus, in the fasted state, python intestinal function is apparently unaffected by surgical transection or resection. Therefore, in the following analyses, we removed the transected treatment and used data only from the resected treatment.

Uptake rates of all four measured solutes differed significantly (P values <0.026) among fasted and postfeeding treatments for each intestinal segment of resected snakes. The proximal and distal segments sig-

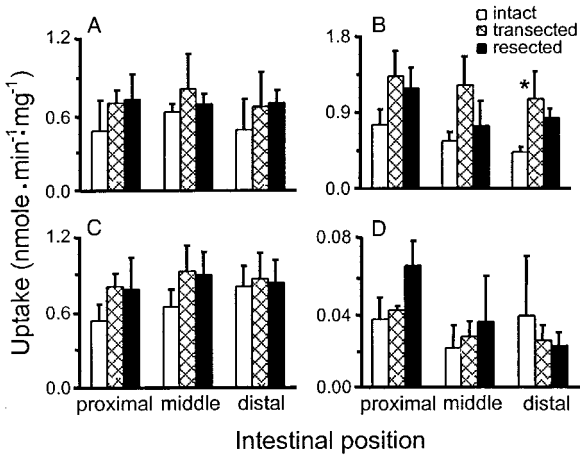

Fig. 1. Intestinal brush-border uptake rates of four nutrients by the proximal, middle, and distal segments of the small intestine from fasted snakes (minimum of 30 days since last meal), with the following 3 intestinal conditions compared: normal intact intestine, surgically transected, and surgically resected. *A*: L-leucine; *B*: L-lysine; *C*: L-proline; *D*: D-glucose. For the transection and resection treatments, the small intestine was severed into equal-length thirds. For transection, the thirds were immediately reconnected in their original position, but for resection the proximal and distal segments were rejoined while the isolated middle segment, retaining its neurovascular supply, was positioned along the reanastomosed intestine. In this and Figs. 2–9, sample size = 3 snakes. Vertical error bars represent means ± SE and are omitted if the bar would be smaller than the symbol for the mean value. Note the lack of treatment-related differences in nutrient uptakes of these fasted pythons. The only significant difference is between intact and transected distal intestine in the uptake of L-lysine (*).

nificantly (P values <0.01 and <0.005, respectively) upregulated uptake of all four nutrients within 24 h of feeding and maintained elevated rates (P values <0.02) through *day 6* (Fig. 2). The only significant declines between *days 1* and *6* were of proximal D-glucose uptake from *days 1* to *4* ($P = 0.027$) and of distal L-lysine uptake from *days 3* to *6* ($P = 0.017$).

In contrast to these proximal and distal results, isolated middle intestinal segments did not significantly increase nutrient uptake rates within 24 or 48 h after feeding, with the one exception of a 4.5-fold increase ($P < 0.0001$) in L-lysine uptake at 2 days (Fig. 2). However, after 3 days of digestion and thereafter, uptake by the isolated intestine for all four nutrients had increased (P values <0.007) from fasting, *day 1*, and *day 2* (for L-leucine, L-proline, and D-glucose) values.

We used previous measures of nutrient uptake from normal intact intestine (no surgical procedure) at 0, 1, 3, and 6 days postfeeding (data used in Ref. 32) to make lateral comparisons with the reanastomosed and isolated segments of the resected intestines of this study. We noted earlier that uptake rates during fasting do not differ between normal intact and resected snakes (Fig. 1). Starting at 1 day postfeeding, nutrient uptake rates were significantly upregulated throughout an intact small intestine (32) and also in the reanastomosed proximal and distal segments of resected snakes (this study; Fig. 2). In lateral comparisons, we found that uptake rates for both the proximal and distal segments of the reanastomosed intestine were on the average higher (5–540% higher) than for the corresponding segments of a normal intact intestine (Fig. 3). Differences were significant (P values <0.05) for the proximal segment at 1 day for L-lysine and at 6 days for L-lysine and L-proline and for the distal segment at 1 and 3 days for L-lysine, L-proline, and D-glucose and at 6 days for L-leucine and L-proline. Because isolated middle segments of resected snakes did not respond functionally within 24 h of feeding, uptake rates of the middle segment of intact snakes at that time were significantly (P values <0.036) greater. At 3 and 6 days, nutrient uptake did not differ between isolated middle segments (having been upregulated) and intact middle segments, with the exception that L-leucine and L-lysine uptake rates were greater (P values <0.025) in isolated segments at 6 days.

Intestinal Nutrient Uptake Capacities

Recall that uptake capacity is the product of uptake rate times intestinal mass, integrated over intestinal length. Uptake capacity of the surgically shortened small intestine increased rapidly after feeding, as a product of the just-mentioned increase in mass-specific uptake rates (Fig. 2) times the about-to-be-mentioned increase in intestinal mass (Fig. 5). For all measured nutrients, intestinal uptake capacities had increased significantly (P values <0.04) within 24 h of feeding and remained elevated through *day 6* (Fig. 4). Compared with our predicted uptake capacities for an intact small intestine (calculated from regression equations and snake body mass; see MATERIALS AND METHODS), the uptake capacities of the reanastomosed intestine were significantly lower (62–83% of predicted values)

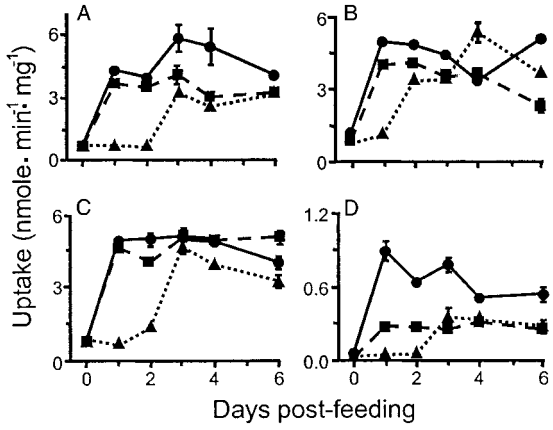

Fig. 2. Intestinal brush-border uptake rates of four nutrients by the proximal (●) and distal (■) remnants of the reanastomosed intestine and by the isolated middle (▲) segment at *day 0* (fasted) and at 1, 2, 3, 4, and 6 days after ingestion of a meal equaling 25–35% of the snake's body mass. L-leucine (*A*), L-lysine (*B*), L-proline (*C*), and D-glucose (*D*) uptake rates, respectively, peaked with 8.1-, 6.5-, 4.3-, and 14-fold increases for the proximal remnant, with 5.9-, 4.9-, 6.1-, and 14-fold increases for the distal remnant, and with 4.7-, 7.2-, 5.2-, and 10-fold increases for the isolated middle segment. Note the upregulation of uptake rates by the proximal and distal remnant by *day 1* and the lack of upregulation by the isolated middle segment until *day 2* or *3*.

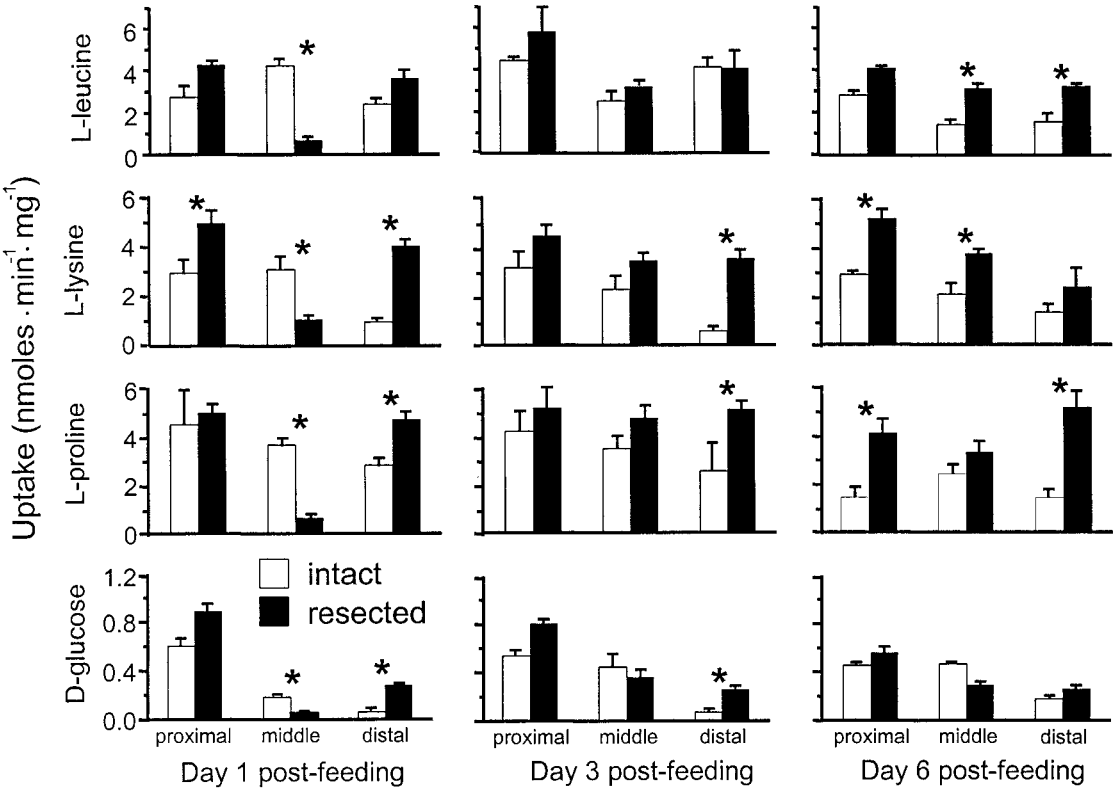

Fig. 3. Comparison between normal intact intestine (open bars) and resected intestine (closed bars) of intestinal brush-border uptake rates of four nutrients in proximal, middle, and distal intestinal segments at 1, 3, and 6 days postfeeding. For resection, the proximal and distal intestinal segments were rejoined by reanatomosis while the isolated middle segment, retaining its neurovascular supply, was left within the body cavity. *Significant differences ($P < 0.05$) between intact and resection treatments. Compared with normal intact intestine, note that resected intestine achieves higher uptake rates in the proximal and distal segments already by *day 1* but that the isolated middle segment has lower uptake rates at *day 1*, because at that time it has been upregulated in intact intestine but not in resected intestine and does not achieve higher values in resected intestine until *day 6*.

at *day 1* for all four nutrients (Fig. 4). At *day 2* and thereafter, uptake capacities for all measured nutrients of the surgically shortened small intestines did not differ significantly from predicted capacities for intact intestines (Fig. 4).

Morphological Response

Intestinal wet mass. Wet masses (mg/cm) of the proximal and distal remnants of the shortened intestine had increased significantly ($P < 0.017$; by 60 and 75%, respectively) with 24 h of feeding and peaked at *day 6* at 2.40 and 2.14 times respective fasting values (Fig. 5*A*). In contrast, isolated middle segments experienced no postfeeding changes in wet mass. As a result, although proximal and middle segments of intact intestine are generally equal to each other in mass (mg/cm), proximal intestinal segments of resected intestine were significantly (P values <0.003) heavier (by as much as 125%) than the isolated middle segments. The distal segment, normally of lower mass than either the proximal and middle segments (32), on average, was heavier than the isolated middle segment at each postfeeding period, significantly so (P values <0.017) at *days 1* and *6*.

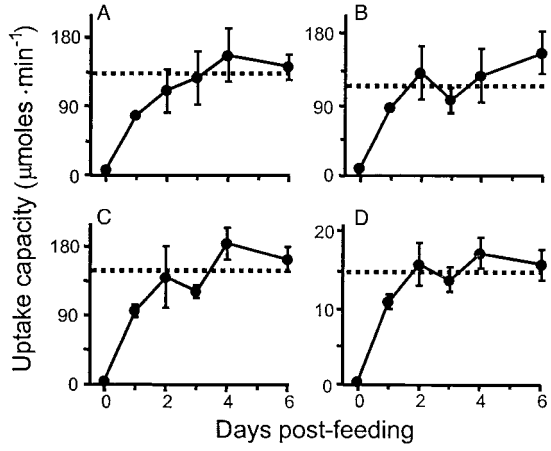

Fig. 4. Intestinal uptake capacities (μmol/min) of four nutrients by the combined proximal and distal segments of the reanastomosed intestine at *day 0* and at 1, 2, 3, 4, and 6 days postfeeding. Uptake capacities are rapidly upregulated after feeding and peak at 20, 14, 20, and 30 times fasting values for L-leucine (*A*), L-lysine (*B*), L-proline (*C*), and D-glucose (*D*), respectively. For each nutrient, the horizontal dotted line illustrates the predicted uptake capacity for that snake's normal intact intestine (calculated from regression of uptake capacities for normal intact intestine against snake body mass). Note that uptake capacities of all nutrients in shortened intestines (two-thirds of original length) reach levels predicted for normal full-length intestines within 2 days postfeeding.

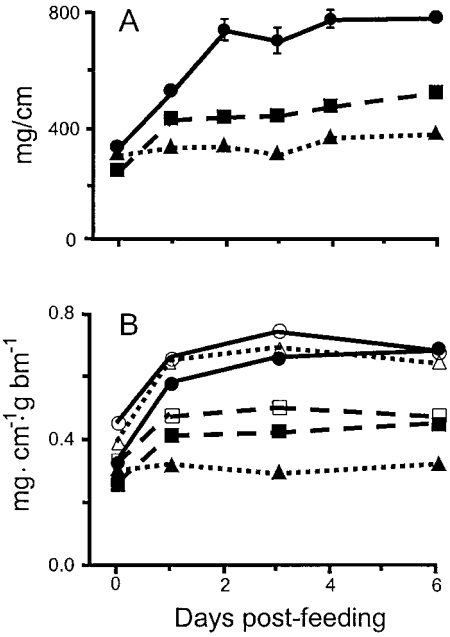

Fig. 5. *A*: wet masses (mg/cm) of the proximal (●) and distal (■) segments of the reanastomosed intestine and of the isolated middle segment (▲) from 0 to 6 days postfeeding. *B*: comparison of wet masses of each intestinal segment ($mg \cdot cm^{-1} \cdot g$ body $mass^{-1}$) between normal intact intestines (○, □, △) and reanastomosed intestines with isolated middle segments (●, ■, ▲). Note the postfeeding increase in intestinal wet mass for all segments except the isolated middle segment.

In analogy to our lateral comparison of nutrient uptake rates, we compared wet masses of normal intact and resected intestinal segments at 0, 1, 3, and 6 days postfeeding. It turned out that the reanastomosed proximal and distal segments did not differ in wet mass from the corresponding segments of intact intestine at any sampling time (Fig. 5*B*). The isolated middle segment of resected intestine did not differ in wet mass from intact intestine during fasting (*day 0*), but at 1, 3, and 6 days it averaged significantly (P values <0.005) lighter (by 50–58%; because the intact, but not the isolated, middle segment increased in mass after feeding).

Enterocyte dimensions. Enterocyte height, width, and volume differed significantly (P values <0.011) among fasted and postfeeding times for both the proximal and distal remnant intestine (Fig. 6). Significant increases in all three of these measures of enterocyte size for these two segments were achieved within 24 h after feeding, most notably with a threefold increase in volume of proximal enterocytes. Enterocytes of the isolated middle segment differed significantly ($P = 0.021$) only in volume among trials (no significant treatment effects on either height or width), experiencing a modest 30% increase by 2 days postfeeding. Although enterocyte size measures did not differ among intestinal segments during fasting, all three size measures were significantly (P values <0.015) larger in the proximal (*days 1–6*) and distal (*days 2–6*) segments than in the isolated middle segment after feeding.

Microvillus length. Microvilli of the proximal segment increased more than fivefold in length ($P = 0.0007$) within 24 h of feeding and remained significantly greater than fasting values (P values <0.005) through *day 6* (Fig. 7). Although overall there was no significant variation among pre- and postfeeding samples in microvillus length for the isolated middle segment, microvillus length was significantly (P values <0.048) greater at 3 and 4 days than during fasting. At each time point, proximal segments possessed significantly longer microvilli than isolated middle segments (P values <0.024).

Enterocyte proliferation. The percentage of enterocytes labeled with the PCNA antibody, indicating cellular proliferation, significantly increased within 24 h after feeding (Fig. 8). For both the proximal and distal segments, proliferation rates remained significantly elevated throughout digestion, peaking at 2 days with 8- and 4.5-fold increases, respectively, over fasting values. The isolated middle segment also experienced significant ($P = 0.016$) variation in proliferation but with only a 2.3-fold increase at 2 days. For each postfeeding period (but not during fasting), proliferation rates were significantly (P values <0.022) greater in the proximal and distal segments than in the isolated middle segment.

Masses of Other Organs

Concurrent with the postprandial growth of the reanastomosed small intestine, wet masses of the liver,

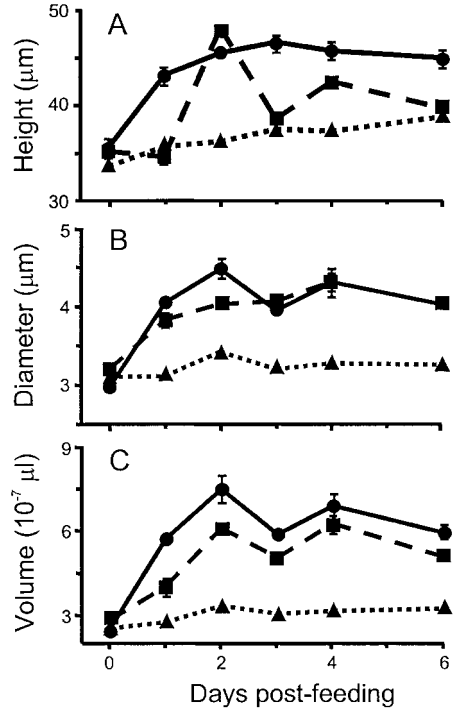

Fig. 6. Enterocyte height (*A*), diameter (*B*), and volume (*C*) for the proximal (●) and distal (■) segments of the reanastomosed intestine and for the isolated middle segment (▲) at *day 0* (i.e., fasted) and at 1–6 days postfeeding. Note the postfeeding increases in enterocyte dimensions for the proximal and distal segments and lack of such increases for the isolated middle segment.

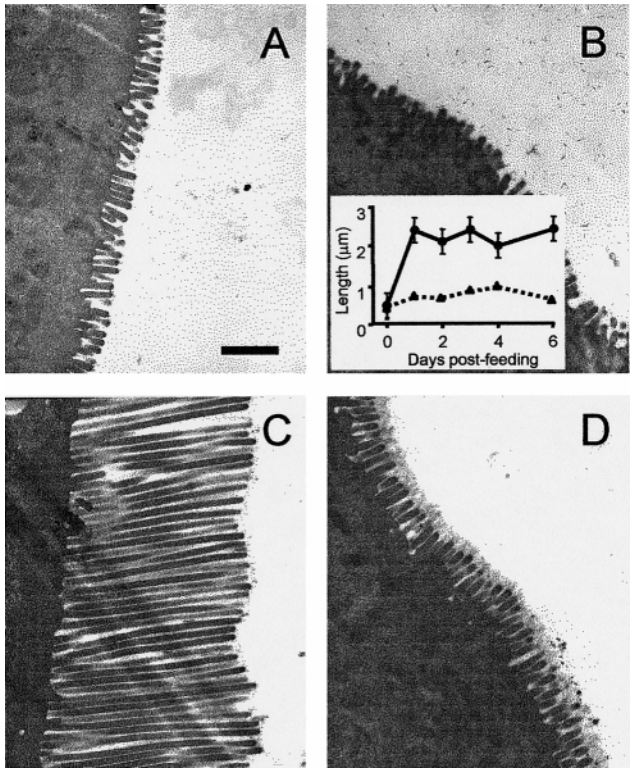

Fig. 7. Electron micrographs of intestinal microvilli from the reanastomosed proximal segment (*A*) and from the isolated middle segment (*B*) of a fasted python and from the reanastomosed proximal segment (*C*) and isolated middle segment (*D*) of a python at 3 days postfeeding. *Inset* in *B* shows microvillus length (μm) of the proximal (●) and isolated middle (▲) segments as a function of time postfeeding. The bar in *A* represents 1 μm. Note the 5-fold increase in microvillus length after feeding in the proximal remnant of the reanastomosed intestine (*C* vs. *A*) and the lack of such a growth response in the isolated middle segment (*D* vs. *B*).

stomach, pancreas, large intestine, and paired kidneys increased significantly (P values <0.04) after feeding (Fig. 9). Postfeeding peaks in the wet masses of these organs occurred, respectively, at 4, 1, 3, 1, and 4 days at values 116, 23, 84, 42, and 45% above fasted values.

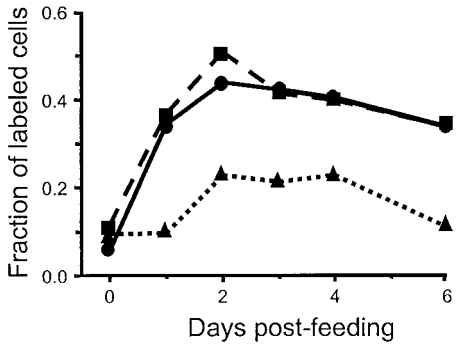

Fig. 8. The fraction of enterocytes undergoing proliferation in the proximal (●) and distal (■) segments of the reanastomosed intestine and for the isolated middle segment (▲) at *day 0* and at 1–6 days postfeeding, as determined by labeling with an antibody for proliferating cell nuclear antigen (PCNA). Note the 8- and 4.5-fold postfeeding increases in cell proliferation for the proximal and distal segments, respectively, but only a 2-fold increase for the isolated middle segment.

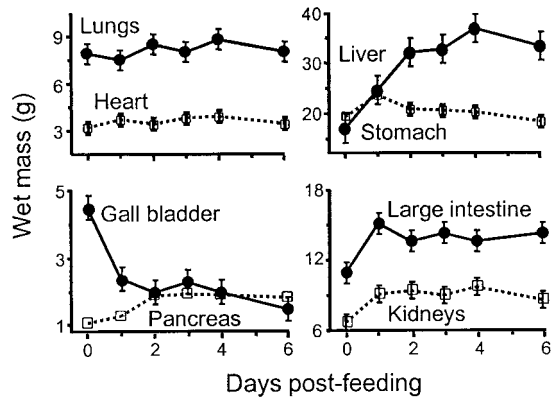

Fig. 9. Wet masses (g) of the lungs, heart, liver, stomach, full gallbladder, pancreas, large intestine, and kidneys at *day 0* and at 1–6 days postfeeding for pythons with reanastomosed proximal and distal small intestine and isolated middle small intestine. Note the postfeeding increases in the wet masses of the liver, stomach, pancreas, large intestine, and kidneys, the significant postfeeding decline in the wet mass of the gallbladder (due to emptying), and the lack of changes in the lungs and heart.

In contrast, the wet mass of the gallbladder and its contents decreased ($P = 0.0001$) by 65% postprandially as bile was released into the small intestine. Dry mass changes generally paralleled these wet mass changes. There were no mass changes in the lungs and heart.

DISCUSSION

Principal Findings

Finding 1. Within 24 h after feeding, the reanastomosed proximal and distal intestinal segments upregulate their nutrient uptake capacities by a factor of 10–30, this factor being a product of 2-fold increases in mucosal mass times 4- to 14-fold increases in mass-specific nutrient uptake rates (Figs. 2–5).

Finding 2. A day later, at 2 days after feeding, the reanastomosed proximal and distal segments, although only two-thirds as long as the original intact intestine, have attained the uptake capacities of an intact intestine at the same time after feeding by further increasing mass-specific nutrient uptake rates (Fig. 4).

Finding 3. In contrast, the isolated middle segment, with its neurovascular attachments intact but cut off from contact with intraluminal nutrients and PB secretions, exhibits no morphological changes (in mucosal mass) nor functional changes (in uptake rates) within 24 h (Figs. 2–6).

Finding 4. Subsequently, however, by 3 days after feeding, the isolated middle segment upregulates uptake rates to equal those of the same segment in an intact intestine at the same time after feeding (Figs. 2 and 3).

Finding 5. Despite this delayed functional response, the isolated middle segment never responds morphologically, even at 6 days after feeding; it retains the appearance of fasted intestine (Figs. 5–7).

Potential Signals and Agents for Gastrointestinal Regulation in Pythons

Much is already known about the signals and agents regulating digestion in mammals (21, 42). Do the same types of signals and agents exist in pythons? As summarized below, the answer is yes.

In mammals a cephalic phase of digestion mediated by the vagus nerve is known to stimulate the secretion of saliva, gastric acid, and pancreatic enzymes (39). In pythons, a corresponding cephalic phase of digestion could be initiated by the python's smelling, seeing, attacking, constricting, and swallowing a prey animal.

As for a gastric phase, the mammalian esophagus and stomach possess stretch-sensitive afferent nerves that stimulate gastric, pancreatic, and intestinal secretion, intestinal transport, and gut motility and blood flow (8, 37). Such a gastric phase could operate easily in pythons, which swallow prey whose diameter is 10 times that of their undistended esophagus and several times that of their undistended stomach.

As for an intestinal phase in mammals, intestinal luminal nutrients trigger the upregulation of their own transporters (12); luminal amino acids contribute to mucosal hypertrophy by being incorporated into enterocyte proteins (3); and the dietary polyamines spermidine and spermine stimulate mucosal growth (23). These processes could also operate in pythons, which experience a huge influx of digesta high in amino acids from the stomach into the intestine.

These comments about the cephalic, gastric, and intestinal phases of digestion all involve ultimate stimuli, which must be translated into proximate regulatory agents. Among such agents identified in mammals (7, 12, 43), postprandial releases of PB secretions and of hormones have been documented in pythons. Bile release and pancreatic enzyme production increase in fed pythons (32, 34), which also experience up to 50-fold increases in plasma levels of the hormones CCK, insulin, gastric inhibitory polypeptide (GIP), neurotensin, and pancreatic glucagon (1, 34).

Actual Agents for Gastrointestinal Regulation in Pythons

The preceding section asked which types of signals and agents regulating digestion in mammals also exist in pythons. Our experiments, in addition, provide some evidence as to which particular digestive responses in pythons are controlled by which types of signals and agents.

First, it is striking that within 24 h of feeding the reanastomosed proximal and distal intestine of pythons responds both morphologically (by an increase in mucosal mass) and functionally (by an increase in transporter activities) but that simultaneously the isolated middle segment responds in neither way. What might account for this difference? The principal difference between the reanastomosed intestine and the isolated middle segment is that the former is exposed to luminal nutrients and PB secretions but the latter is exposed to neither. Hence luminal nutrients, PB secretions, or both may be the proximate agents responsible for intestinal mucosal growth within 24 h in pythons.

Second, the isolated middle segment of pythons does respond with upregulation of transporter activities by 3 days after feeding. Because the isolated middle segment receives no luminal nutrients or PB secretions that could trigger this response, the proximate agents must instead be nerves and/or hormones. Evidence for such a regulatory role in mammals includes increased cell proliferation and DNA and RNA content in Thiry-Vella fistulas of rat intestine that have also been subjected to major resection (15, 44). Three lines of evidence implicate a regulatory role, specifically of hormones in mammals: *1*) an increase in plasma and/or tissue levels of seven gastrointestinal hormones [CCK, enteroglucagon, gastrin, glucagon-like peptide (GLP)-1, GIP, pancreatic polypeptide, and peptide YY] and two growth factors [epidermal growth factor (EGF) and insulin-like growth factor (IGF)] after intestinal resection in rodents and dogs (2, 15, 27, 30, 38, 46); *2*) that the administration of any of four gastrointestinal hormones (CCK, GLP-2, pentagastrin, or secretin) or three growth factors [EGF, IGF, or keratinocyte growth factor (KGF)], operating individually and synergistically with growth hormone and the nutrient glutamine, prevents the hypoplasia and functional downregulation of rat intestine otherwise observed during total parenteral nutrition (TPN; see Refs. 6, 14, 18, 20, 22, 28, 29); and *3*) that the administration of GLP-2, neurotensin, EGF, IGF, or KGF augments mucosal hyperplasia after intestinal resection in rats (5, 19, 24, 26, 31). As we already mentioned, at least five gastrointestinal hormones undergo postprandial rises in plasma levels in pythons (1, 34).

Finally, what scenario could account for the delay in the response of the isolated middle segment, i.e., transporter upregulation by *day 3* but not by *day 1*? Reflect that the reanastomosed proximal and distal segments are 33% shorter than the normal intestine, that their combined uptake capacities are as a result lower than those of a normal intestine at *day 1*, and their uptake capacities do not increase to equal those of a normal intestine until *day 2* (Fig. 4). One therefore expects that more nonabsorbed nutrients than usual are entering the distal intestine during the first day or two of digestion. Studies in mammals show that proglucagon-derived peptides (PGDPs, including enteroglucagons, GLP-1, and GLP-2) are produced in the ileum and colon (42) and that they are released in response to luminal nutrient overload there (4). It has been implicated further that it is GLP-2 that mediates the adaptive responses (mucosal growth and slowing of transit time) of resected mammalian intestine (10, 31). Perhaps, for pythons, the delayed distal nutrient overload (first occurring 2 days after feeding) and subsequent hormone release are, respectively, the signal and the agent accounting for the delayed responses of the isolated middle intestinal segment to upregulate nutrient transport and for the reanastomosed intestine to further upregulate nutrient uptake. Identification of whether there exist a homologous performance-en-

hancing hormone to mammalian PGDPs (specifically GLP-2) in pythons awaits future study.

Comparison of Response Mechanisms Between Pythons and Mammals

Although we have noted many similarities between pythons and mammals in digestive physiology, there are of course also some differences. Three differences stand out.

First, mammalian intestine deprived of nutrients (e.g., a Thiry-Vella fistula, a bypassed loop attached distally to the intestinal lumen, or the whole intestine during TPN) exhibits hypoplasia, entailing as much as a 70% reduction in mucosal mass, protein, and DNA and a 40% reduction in villus height and cellular proliferation rates (6, 15, 29, 45). No such reduction below fasting levels is observed in bypassed middle segments of python intestine. Perhaps that is because fasts in pythons normally last several weeks or months, so that fasting python intestine already has its mass regressed as far as it can regress.

Second, the response of bypassed mammalian loops (only in conjunction with major resection) to feeding involves mucosal growth (35% increase in mass with a 75% resection; see Ref. 15) and no functional response (17). In contrast, the response in bypassed python loops is mainly functional (transporter upregulation) rather than morphological.

Finally, essentially that same difference between pythons and mammals applies to their responses to intestinal resection. In both species, an intestine whose length has been shortened by experimental resection undergoes compensatory changes to restore functional capacities equal to those of the original full-length intestine. In mammals, those compensatory changes consist of increases in mucosal mass (as much as 100%/length; see Ref. 11) arising from as much as a 30% increase in enterocyte proliferation (17) and 30–60% increases in villus height and crypt depth (11, 45). In pythons, however, the changes involve further upregulation of mass-specific nutrient transport rates. This is most obvious in the distal portion of the reanastomosed intestine, where nutrient uptake rates average 180% greater than rates in the same region of the intact intestine (32). Unlike mammalian intestine, remnant python intestine appears unable to undergo further mucosal growth beyond levels normally experienced with the ingestion of a meal, perhaps because mucosal growth associated with a normal meal is already so great in pythons. Hence any further increase in functional capacity can only be achieved by further upregulating nutrient transporter activities. Similarly, when pythons consume a prey animal equivalent to 65% of their own body mass, we noted no further increase in intestinal mass beyond that observed in pythons digesting a meal equivalent to "only" 25% of their own body mass, but we did observe further increases in mass-specific nutrient transport rates (33).

Advantages of the Python Model

Naturally, we do not assume that gastrointestinal regulation proceeds identically in pythons and in humans or other mammals nor that findings about pythons can be transferred immediately to humans without further testing. Indeed, we have noted some differences between pythons and rats with respect to gastrointestinal regulation, and other studies have noted differences between rats and humans. Instead, the rationale for using pythons, rats, or other animal models is that identification of mechanisms in some easily studied species (e.g., pythons or rats) may make it easier to design experiments for efficiently identifying mechanisms in some harder-to-study species (e.g., humans).

Our results suggest six advantages warranting further study of the python model.

Advantage 1. Because juvenile pythons are gentle, feed and defecate at intervals of several weeks or more, spend most of their time coiled up and quiescent, and do not bite unless drastically provoked, pythons are far easier and safer to maintain and care for than are rats and other laboratory mammals.

Advantage 2. Again, because of their long natural feeding intervals, pythons can be left for weeks or months without feeding to heal after gut surgery. In contrast, mammals require either oral food or else TPN within days of gut surgery. This difference may contribute to the low frequency of postoperative complications that we observed in our pythons compared with mammals after intestinal resection (no deaths or complications in any of our 21 pythons).

Advantage 3. Pythons and their internal organs are long, slender, relatively straight, and aligned in parallel. Mammals are more round, have highly coiled intestines, and have complex relative positions of other viscera. Intestinal surgery on pythons is facilitated by their linear anatomy and relatively large intestines.

Advantage 4. Regulatory spans for mucosal growth and for intestinal transporter activities are much larger in pythons than in laboratory mammals.

Advantage 5. Mucosal growth and transporter responses associated with intestinal resection are more rapid in pythons than in laboratory mammals. Within 24 h of feeding, the reanastomosed python intestine has doubled in mass and has upregulated nutrient transporter activities by 4- to 14-fold, and its nutrient transporter capacities have increased to compensate for resection within 2 days. Even the isolated middle segment upregulates transporter activities 10-fold within 3 days. In contrast, mammalian models take several weeks after intestinal resection to reach peaks in intestinal responses (43).

Advantage 6. In resected mammalian models, mucosal growth precedes or accompanies transporter upregulation, making it difficult to study mechanisms of transporter regulation without the complications introduced by concomitant mucosal growth. In contrast, the isolated middle segment of python intestine responds only by transporter upregulation. This may make it

easier to identify the underlying mechanisms. For all of these reasons, python intestine recommends itself for further surgical studies.

We thank D. Do, C. Entwisle, J. Issacs, J. Johns, K. Kim, L. Pham, S. Sampogna, K. Searcy, D. Secor, B. Sjostrand, C. Slotnick, S. Szabo, R.Torres, and F. Wayland for help with experiments.

This work was supported by National Institutes of Health Research Service Award DK-08878 and Grant GM-14772.

Present addresses: S. M. Secor: Dept. of Biology, University of Mississippi, University, MS 38677-1848; E. E. Whang and S. W. Ashley: Dept. of Surgery, Brigham and Women's Hospital, Harvard University, Boston, MA 02115.

REFERENCES

1. **Adrian TE, Secor S, Staab P, Fehsenfeld D, and Diamond J.** Gastrointestinal hormone changes and the bowel adaptation associated with feeding in the Burmese python (Abstract). *Gastroenterology* 100: A1005, 1996.
2. **Adrian TE, Thompson JS, and Quigley EM.** Time course of adaptive regulatory peptide changes following massive small bowel resection in the dog. *Dig Dis Sci* 41: 1194–1203, 1996.
3. **Alpers DH.** Protein synthesis in intestinal mucosa: the effect of route of administration of precursor amino acids. *J Clin Invest* 51: 167–173, 1972.
4. **Bristol JB, Williamson RCN, and Chir M.** Nutrition, operations, and intestinal adaptation. *J Parenter Enteral Nutr* 12: 299–309, 1988.
5. **Chaet MS, Arya G, Ziegler MM, and Warner BW.** Epidermal growth factor enhances intestinal adaptation after massive small bowel resection. *J Pediatr Surg* 29: 1035–1039, 1994.
6. **Chance WT, Foley-Nelson T, Thomas I, and Balasubramaniam A.** Prevention of parenteral nutrition-induced gut hypoplasia by coinfusion of glucagon-like peptide-2. *Am J Physiol Gastrointest Liver Physiol* 273: G559–G563, 1997.
7. **Chen YF, Feng ZT, Wen SH, and Lu GJ.** Effect of vasoactive intestinal peptde, somatostatin, neurotensin, cholecystokinin octapeptide, and secretin on intestinal absorption of amino acid in rats. *Dig Dis Sci* 32: 1125–1129, 1987.
8. **Cooke HJ and Reddix RA.** Neural regulation of intestinal electrolyte transport. In: *Physiology of the Gastrointestinal Tract*, edited by Johnson LR. New York: Raven, 1994, p. 2083–2132.
9. **Dietrich DR.** Toxicological and pathological applications of proliferating cell nuclear antigen (PCNA), a novel endogenous marker for cell proliferation. *Crit Rev Toxicol* 23: 77–109, 1993.
10. **Drucker DJ, Ehrlich P, Asa SL, and Brubaker PL.** Induction of intestinal epithelial proliferation by glucagon-like peptide 2. *Proc Natl Acad Sci USA* 93: 7911–7916, 1996.
11. **Fenyö G, Hallberg D, Soda M, and Roos KA.** Morphological changes in the small intestine following jejuno-ileal shunt in parenterally fed rats. *Scand J Gastroenterol* 11: 635–640, 1976.
12. **Ferraris RP and Diamond J.** Regulation of intestinal sugar transport. *Physiol Rev* 77: 257–302, 1997.
13. **Gershon MD, Kirchgessner AL, and Wade PR.** Functional anatomy of the enteric nervous system. In: *Physiology of the Gastrointestinal Tract*, edited by Johnson LR. New York: Raven, 1994, p. 381–422.
14. **Goodlad RA, Mandir N, Meeran K, Ghatei MA, Bloom SR, and Playford RJ.** Does the response of the intestinal epithelium to keratinocyte growth factor vary according to the method of administration? *Regul Pept* 87: 83–90, 2000.
15. **Gornacz GE, Ghatei MA, Al-Mukhtar MYT, Yeats JC, Adrian TE, Wright NA, and Bloom SR.** Plasma enteroglucagon and CCK levels and cell proliferation in defunctioned small bowel in the rat. *Dig Dis Sci* 29: 1041–1049, 1984.
16. **Hammond KA, Lam M, Lloyd KCK, and Diamond J.** Simultaneous manipulation of intestinal capacities and nutrient loads in mice. *Am J Physiol Gastrointest Liver Physiol* 271: G969–G979, 1996.
17. **Hanson WR, Rijke RPC, Plaisier HM, Van Ewijk W, and Osborne JW.** The effect of intestinal resection on thiry-vella fistulae of jejunal and ileal origin in the rat: evidence for a systemic control mechanism of cell renewal. *Cell Tissue Kinet* 10: 543–555, 1977.
18. **Hughes CA, Bates T, and Dowling RH.** Cholecystokinin and secretin prevent the intestinal mucosal hypoplasia of total parenteral nutrition in the dog. *Gastroenterology* 75: 34–41, 1978.
19. **Izukura M, Evers BM, Parekh D, Yoshinaga K, Uchida T, Townsend CM, and Thompson JC.** Neurotensin augments intestinal regeneration after small bowel resection in rats. *Ann Surg* 215: 520–526, 1992.
20. **Jacob DO, Evans DA, Mealy K, O'Dwyer ST, Smith RJ, and Wilmore DW.** Combined effects of glutamine and epidermal growth factor on the rat intestine. *Surgery* 104: 358–364, 1988.
21. **Johnson LR.** *Gastrointestinal Physiology*. St. Louis, MO: Mosby, 1997.
22. **Johnson LR, Lichtenberger LM, Copeland EM, Dudrick SJ, and Castro GA.** Action of gastrin on gastrointestinal structure and function. *Gastroenterology* 68: 1184–1192, 1975.
23. **Johnson LR and McCormack SA.** Regulation of gastrointestinal mucosal growth. In: *Physiology of the Gastrointestinal Tract*, edited by Johnson LR. New York: Raven, 1994, p. 611–641.
24. **Johnson WF, DiPalma CR, Ziegler TR, Scully S, and Farrell CL.** Keratinocyte growth factor enhances early gut adaptation in a rat model of short bowel syndrome. *Vet Surg* 29: 17–27, 2000.
25. **Karasov WH and Diamond JM.** A simple method for measuring intestinal solute uptake in vitro. *J Comp Physiol* 152: 105–116, 1983.
26. **Lemmey AB, Martin AA, Read LC, Tomas FM, Owens PC, and Ballard FJ.** IGF-I and the truncated analogue des-(1—3)IGF-I enhance growth in rats after gut resection. *Am J Physiol Endocrinol Metab* 260: E213–E219, 1991.
27. **Lilja P, Wiener I, Inoue K, and Thompson JC.** Changes in circulating levels of cholecystokinin, gastrin, and pancreatic polypeptide after small bowel resection in dogs. *Am J Surg* 145: 157–162, 1983.
28. **Marchbank T, Goodlad RA, Lee CY, and Playford RJ.** Luminal epidermal growth factor is trophic to the small intestine of parenterally fed rats. *Clin Sci (Colch)* 89: 117–120, 1995.
29. **Peterson CA, Carey HV, Hinton PL, Lo H-C, and Ney DM.** GH elevates serum IGF-I levels but does not alter mucosal atrophy in parenterally fed rats. *Am J Physiol Gastrointest Liver Physiol* 272: G1100–G1108, 1997.
30. **Roundtree DB, Ulshen MH, Selub S, Fuller CR, Bloom SR, Ghatei MA, and Lund PK.** Nutrient-independent increases in proglucagon and ornithine decarboxylase messenger RNAs after jejunoileal resection. *Gastroenterology* 103: 462–468, 1992.
31. **Scott RB, Kirk D, MacNaughton WK, and Meddings JB.** GLP-2 augments the adaptive response to massive intestinal resection in rat. *Am J Physiol Gastrointest Liver Physiol* 275: G911–G921, 1998.
32. **Secor SM and Diamond J.** Adaptive responses to feeding Burmese pythons: pay before pumping. *J Exp Biol* 198: 1313–1325, 1995.
33. **Secor SM and Diamond J.** Effects of meal size on postprandial responses in juvenile Burmese pythons (*Python molurus*). *Am J Physiol Regulatory Integrative Comp Physiol* 272: R902–R912, 1997.
34. **Secor SM and Diamond J.** A vertebrate model of extreme physiological regulation. *Nature* 395: 659–662, 1998.
35. **Secor SM, Stein ED, and Diamond J.** Rapid upregulation of snake intestine in response to feeding: a new model of intestinal adaptation. *Am J Physiol Gastrointest Liver Physiol* 266: G695–G705, 1994.
36. **Seelig LL, Winborn WB, and Weser E.** Effect of small bowel resection on the gastric mucosa in the rat. *Gastroenterology* 72: 421–428, 1977.
37. **Sengupta JN and Gebhart GF.** Gastrointestinal afferent fibers and sensation. In: *Physiology of the Gastrointestinal Tract*, edited by Johnson LR. New York: Raven, 1994, p. 483–519.
38. **Shin CE, Falcone RA, Duane KR, Erwin CR, and Warner BW.** The distribution of endogenous epidermal growth factor after small bowel resection suggests increased intestinal utilization during adaptation. *J Pediatr Surg* 34: 22–26, 1999.

39. **Solomon TE.** Control of exocrine pancreatic secretion. In: *Physiology of the Gastrointestinal Tract*, edited by Johnson LR. New York: Raven, 1994, p. 1499–1529.
40. **Stevens BR, Ross HJ, and Wright EM.** Multiple transport pathways for neutral amino acids in rabbit jejunal brush border vesicles. *J Membr Biol* 66: 213–225, 1982.
41. **Urban E, Michel AM, and Weser E.** Dissociation of mucosal mass and adaptive change in electrolyte, water and sugar transport in rats after intestinal resection. In: *Mechanisms of Intestinal Adaptation*, edited by Robinson JWL, Dowling RH, and Riecken E-O. Lancaster, PA: MTP, 1981, p. 529–541.
42. **Walsh JH.** Gastrointestinal hormones. In: *Physiology of the Gastrointestinal Tract*, edited by Johnson LR. New York: Raven, 1994, p. 1–128.
43. **Weser E, Heller R, and Tawil T.** Stimulation of mucosal growth in the rat ileum by bile and pancreatic secretions after jejunal resection. *Gastroenterology* 73: 524–529, 1977.
44. **Williamson RCN and Bauer FLR.** Evidence for an enterotropic hormone: compensatory hyperplasia in defunctioned bowel. *Br J Surg* 65: 736–739, 1978.
45. **Williamson RCN, Bauer FLR, Ross JS, and Malt RA.** Proximal enterectomy stimulates distal hyperplasia more than bypass or pancreaticobiliary diversion. *Gastroenterology* 74: 16–23, 1978.
46. **Wiren M, Adrian TE, Arnelo U, Permert J, Staab P, and Larsson J.** An increase in mucosal insulin-like growth factor II content in postresectional rat intestine suggests autocrine or paracrine growth stimulation. *Scand J Gastroenterol* 33: 1080–1086, 1998.